Scientific Journal of King Faisal University:
Basic and Applied Sciences

Comparison of Various Tree Features for Blocking Solar Radiation in the Arid Urban Environment

Abdullah M. Farid Ghazal

Department of Landscape Architecture, Faculty of Architecture and Planning, King Abdulaziz University, Jeddah, Saudi Arabia

LINK	RECEIVED	ACCEPTED	PUBLISHED ONLINE	ASSIGNED TO AN ISSUE
https://doi.org/10.37575/eng/230049	08/10/2023	04/01/2024	04/01/2024	01/06/2024

NO. OF WORDS	NO. OF PAGES	YEAR	VOLUME	ISSUE
7141	7	2024	25	1

ABSTRACT

In the arid urban environment, pedestrians are often exposed to high amounts of solar radiation during summer, which can limit their activities. Shades are essential for reducing the harmful effects of solar radiation, particularly ultraviolet (UV) rays, which can be dangerous to human health. This study thoroughly evaluated the effect of various tree features for their efficacy in blocking solar radiation, especially photosynthetically active radiation (PAR) and ultraviolet A (UVA). Tree height, trunk height, canopy height and diameter, leaf area index (LAI), leaf size and type, planting techniques (individual and cluster), and agriculture services for eight common tree species used in the Landscape at King Abdulaziz University campus in Jeddah, KSA, were examined. Measurements were taken at noon when the solar zenith angle was perpendicular. The study found that the ability to block PAR and UVA varies based on several factors analyzed. Canopy height and diameter increased a tree's capability to block radiation, with pyramid-shaped trees and simple leaves being the most effective. Higher LAI, cluster planting, and removal of lower branches also increased a tree's radiation-blocking power. In conclusion, shade trees mitigate PAR and UVA and provide pedestrians with more opportunities to enjoy open landscapes in arid regions.

KEYWORDS

landscape planting, leave index, solar effect, trees benefits, ultraviolet radiation, arid environments

CITATION

Ghazal, A.M.F. (2024). Comparison of various tree features for blocking solar radiation in the arid urban environment. *Scientific Journal of King Faisal University: Basic and Applied Sciences*, **25**(1), 6 – 12. DOI: 10.37575/eng/230049

1. Introduction

Trees serve different purposes, such as aesthetic, functional, and environmental, in urban environments. The urban environment is influenced by using trees that improve the quality of life and create an eco-friendly and sustainable urban environment, especially in arid regions; it provides better environmental services and appropriate conditions for users in harmony with seasonal changes (Morakinyo *et al.,* 2016). Trees can help to modify the air temperature, cooling the air, increase air humidity, reduce wind speed, produce oxygen, save energy, reduce stormwater, mitigate air pollution, abate noise, and modify air pollutants (De-Abreu-Harbich *et al.,* 2015; Parker and Simpson, 2020). Moreover, it is worth noting that trees provide better shade than pergolas by helping to reduce all types of solar radiation (SR).

1.1. Types of Solar Radiation and their Environmental Effects:

There are three main types of SR: ultraviolet, visible light, and infrared. Ultraviolet radiation (UVR) consists of three types: UVA bandwidth (315–400 nanometres [nm]), UVB bandwidth (280–315 nm), and UVC bandwidth (100–280 nm). UVR consists of 5% of the total SR of the Earth (Modenese *et al.,* 2018). The photosynthetically active radiation (PAR), which corresponds to the range of visible light to the human eye, extends from a bandwidth of about 400 to 700 nm; it has about 50% of the SR on the Earth's surface. It is a surrogate for visible light measurements (Grant and Heisler, 2001; Heisler *et al.*, 2003). Infrared radiation (IR) is 700–3000 nm, sometimes called infrared light. It further subdivides into IR-A bandwidth (780–1400 nm), IR-B bandwidth (1400–3000 nm), and IR-C bandwidth (1 mm–3000 nm), which comprises 45% of SR (Modenese *et al.,* 2018).

The amount of SR reaching the Earth's surface is determined by many factors such as astronomical physical, geographical, and cloud properties (Boukelia *et al.*, 2014). In general, owing to the atmosphere's filtering effect, the SR to the Earth's surface is composed primarily of frequencies within the IR and the visible radiation and UVR (Modenese *et al.,* 2018*)*. In an urban landscape, SR (such as UVR) is affected by the climatic region, population density, and socioeconomic characteristics; it is blocked and controlled by buildings, trees, and other pergola structures (Grant *et al.*, 2002).

Solar radiation (or SR) has many benefits for those living on Earth. It plays an essential role in human life. Visible light regulates the daily lifecycle between night and day, is an essential source of energy for much of life on this planet and is the vital source of energy to carry out photosynthesis in plants, thereby providing food for all living organisms and energy for all types of terrestrial and sea creatures (Fuller *et al.*, 2015). (IR) plays a significant role in the Earth's surface's heat distribution. Ultraviolet radiation is vital in killing pathogenic bacteria and reducing the spread of diseases (Grant *et al.*, 2002).

1.2. Damage Caused by Radiation to Humans:

It is essential to be aware of the potentially harmful effects of different types of radiation. While visible light may seem harmless in some circumstances, it can cause burning of the skin and damage to the eyes (Environment, Health and Safety, 2018). However, UVR is likely to cause the most severe health effects on humans. UVR causes damage to materials, alters the herbivores nature of insects and the activities of microbes, modifies vegetation growth, and has adverse effects on human health (Heisler *et al.*, 2003; Modenese *et al.,* 2018). UVR and SR have been classified as human carcinogens (Modenese *et al.,* 2016). The IR affects the urban environment and causes changes in climatic conditions. People living in urban areas may experience intense heat stress and hot thermal sensation (Yeo *et al.*, 2021). The best way to mitigate these effects is to increase vegetation cover in these areas, which can mitigate urban heat islands and control microclimate and other ecosystem services (Kong *et al.*, 2017).

1.3. Ultraviolet Radiation:

Each type of UV has a different impact. UVA plays no part in synthesizing vitamin D3 in humans, but it penetrates deep into the

Corresponding Author: Abdullah M. Farid Ghazal 00966506620717, aghazal@kau.edu.sa

skin. It ages the skin but contributes much less towards sunburn, according to the World Health Organization (2016). UVB is responsible for most sunburns, but it hits cholesterol in the skin cells, providing the energy for vitamin D synthesis. Low blood serum vitamin D3 is linked to several types of cancer and severe human diseases (Trumbull and Parisi, 2010). The third type, UVC, could be the most dangerous but is absorbed by ozone, water vapor, oxygen, and carbon dioxide, as per Cancer Research UK (2021). Therefore, seeking practical solutions for mitigating UVR to improve human health in urban environments is imperative (Deng *et al.*, 2020). Many researchers have tried to determine the impact of UVR on human health and habits (Grant *et al.*, 2002; Heisler *et al.*, 2004) in different circumstances, such as the impact on pedestrians (Grant *et al.*, 2002), workers in other conditions (Gies and Wright, 2003; Modenese *et al.*, 2016; Modenese *et al.*, 2018) and even on children in nursery schools (Gies and Mackay, 2004). Research has shown that UVA plays a significant role in causing mutagenic and carcinogenic effects on human skin (Trumbull and Parisi, 2010). Non-melanoma skin cancers are thought to be correlated to cumulative lifetime, UVR exposure (Grant *et al.*, 2002). They can cause melanocyte proliferation, cause abnormalities in DNA, and modify gene expression (Trumbull and Parisi, 2010), such that both types can skin cancer.

1.4. Benefits of Shade:

Most people try to protect themselves from SR by modifying the environment with shade and using protective umbrellas, buildings, vegetation, or personal UVR protective items, such as sun-protective clothing, hats, sunscreens, and sunglasses (Gies and Mackay, 2004). For that, the potential effects of UVR are modified by the shade of trees, which influences UVR exposure to various degrees (Heisler *et al.*, 2003) and significantly minimizes the area of the sky in view. The study by Trumbull and Parisi (2010) found that UVA exposure was reduced by as much as 65% when using a shade umbrella. However, the specific longwave property of UVA enables it to penetrate most automobile, office, and household windows, whereas UVB is blocked by window glass (Trumbull and Parisi, 2010).

It is interesting to learn that ancient cities in dry regions like Jeddah, Damascus, Aleppo, and Cairo had narrow roads, closed buildings, and shelters as the primary shade devices to reduce exposure to SR. However, in modern cities, the areas between buildings, streets, and squares have become oversized, requiring sufficient alternative shade from SR. Shade sites can be achieved by placing shade structures close to buildings or fences, using trees and plants for screening, or partially walling the shade structures (Gies and Mackay, 2004; Grant and Heisler, 2006). Therefore, green infrastructure is a successful alternative to significantly contribute to urban centers (Parker and Simpson, 2020; Zhao *et al.*, 2018). Large trees and multi-layered planting assist in longwave radiation mitigation, more than single-layer planting, by blocking building radiation (Kwon and Lee, 2019).

1.5. Influence of Trees:

Trees are indeed crucial when it comes to blocking different types of solar radiation. They provide a natural barrier that helps filter out harmful rays from the sun, which can damage both humans and the environment. However, the tree species' ability changes according to their canopy properties (Sanusi *et al.*, 2017).

1.5.1. Trees Canopy Features

The influence on SR control, such as thermal and UVR, changes according to the canopy dimensions of height, diameter, and trunk height on the one hand and the leaves' sizes, shapes, and surface structures on the other hand (Grant *et al.*, 2003). These effects have been studied in many types of research (Shahidan *et al.*, 2010; Sanusi *et al.*, 2017; Armson *et al.*, 2013; Grant and Heisler, 2006; Zheng *et al.*, 2018; Kong *et al.*, 2017; TUN and MG 2020; Deng *et al.*, 2020). Furthermore, the benefits of the microclimate of tree canopies may differ in terms of air temperature, relative humidity, SR, mean radiant temperature, and wind speed (Sanusi *et al.*, 2017).

1.5.2. The Leaf Area Index

The Leaf Area Index (LAI) is a well-established measurement parameter in forestry, agriculture, and ecology, LAI is defined as the total projected area of leaves of a single tree or group of trees over a unit of land (TUN and MG, 2020). It is an essential aspect of tree canopies affecting SR penetration and microclimate below canopies (Sanusi *et al.*, 2017; Fahmy *et al.*, 2010). It has been applied in several articles to measure outdoor trees' influence LAI (Deng *et al.*, 2020; Shahidan *et al.*, 2010). On the other hand, LAI was the main driver of tree cooling for outdoor temperature regulation, followed by trunk height, tree height, and crown diameter (Zheng *et al.*, 2018). Hence, it should be a priority to improve the comfort of outdoor environments (Armson *et al.*, 2013; Shahidan *et al.*, 2010).

1.5.3. Planting Design Rules

Planting design is based on multiple rules, such as aesthetic, functional, and environmental criteria. The correct choice of tree species and their location is one of the essential prerequisites for achieving sustainability in planting design in landscape architecture. Therefore, it is necessary to adjust the selection of trees to earn the highest degree of solar radiation control. These can be achieved by comprehending the tree's canopy and leaves properties and suitability for design to control SR in the urban environment (Sanusi *et al.*, 2017; Deng *et al.*, 2020) and the influence of differences between planting trees individually and in groups (Heisler *et al.*, 2003).

The study focuses on analyzing the effectiveness of different tree species in blocking PAR and UVA in an arid region. The aim is to enhance the pedestrian conditions in an open landscape. This research explores the impact of the trees' canopy and shapes of leaves and LAI on the overall performance. Our study highlights the importance of carefully selecting tree species and designing their layout to create a more pleasant and safe pedestrian environment in arid regions.

2. Materials and Methods

2.1. Study Area:

This study was conducted at King Abdulaziz University, KAU, campus (21.29° N, 39.14° E), Jeddah, west of Saudi Arabia. Jeddah is located in the Red Sea coastal area. The rainfall is less than 54 mm/year, and the mean temperature in summer is 31.9 ℃ and goes up to 38.8 ℃ as a maximum. The study area has a period of high solar brightness most of the year, and the clear sky hours range between 76-83% (Table 1).

Table 1: Climate data for Jeddah Temperature, precipitation, and wind speed.

	Temperature °C (1)					Precipitation (mm/year) (1)	Wind velocity (km/h) (1)	Clear sky hours (2)	
	Yearly	Spring	Summer	Autumn	winter	Mean	max	May	Jun
T=Max °C	38.8	34.1	38.2	35.4	30.6	54	118.5	83%	76%
T=Mean °C	28.2	27.7	31.9	29.3	25.0				
T=Min °C	18.1	21.9	26.0	24.1	20.1				

Source: 1: The General Authority of Meteorology and Environmental Protection in KSA. Period: 35 years.
2: weather spark, 2023.

The KAU campus area extends over 6 km^2. It collects more than 100 native and introduced landscape architecture species including more than 30 tree species that provide shade for pedestrians on the sidewalks and squares. Eight tree species with the best mature samples were chosen in this study to complete the measurements for their features,

planting, and agricultural conditions (Table 2) (Figure 1).

Table 2: Plant name, family, number of samples, tree properties (canopy and leaves), and planting of the eight tree species selected.

plant name	Family	Plant codes	No. of samples	Canopy Type	leaf type and size	leaf or leaflet shape	Planting clusters and individual
Ficus virens Aiton =*Ficus altissima* Blume	Moraceae	fnit	12	rounded	simple medium	ovate-elliptic	clusters and individual
Ficus microcarpa var. *nitida* F.C.Ho =*Ficus nitida*Thunb = *Ficus benjamina* L.	Moraceae	falt	12	irregular	simple small	elliptic ovate or obovate	individual
Peltophorum pterocarpum (DC.) Backer	Fabaceae	pelt	15	rounded	bipinnate very small	oblong	clusters and individual
Plumeria obtusa L.	Apocynaceae	plu	6	irregular	simple large	obovate	individual
Millingtonia hortensis L.f.	Bignoniaceae	mill	5	Vase	bipinnate small	deltoids	individual
Conocarpus lancifolius Engl.	Combretaceae	conoc	7	elongated	simple small	oblong-lanceolate	clusters and individual
Polyalthia longifolia (Sonn.) Thwaites	Annonaceae	poly	5	pyramidal	simple medium	elliptic (oval) obovate	individual
Tabebuia roseoalba (Ridl.) Sandwith =*Tabebuia rosea* DC.	Bignoniaceae	tab	8	elongated	Palmately medium	oval	individual

Figure 1: The tree form types, planting groups, and leaves measurements of the eight tree species studied.

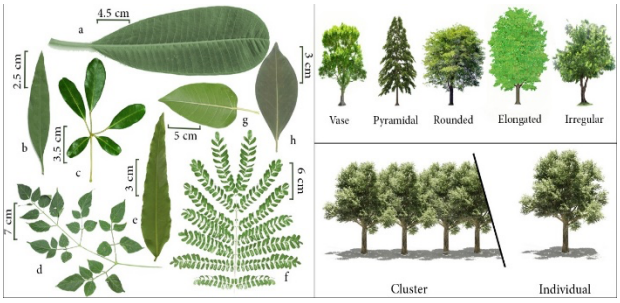

2.2. Types of Measurements:

Jeddah is near the Tropic of Cancer at 21.29° N and 39. 14° E and this situation constituted a vital opportunity to carry out this research, allowing us to focus on determining the differences between the tree canopies blocking PAR and UVA without impacting the sun's position on the tree canopies. The solar zenith angle SZA θ is almost perpendicular (θ = 88°–90°) at noontime (12:00–13:00) in the period from 01-June to 15- July 2022 (Fig 2).

The data collected for the eight studied species of trees included measurements for tree height H_{tree}, tree canopy diameter D_{canopy}, canopy height H_{canopy}, and trunk height H_{trunk} (Figure 2). Information about the trees' morphological features (canopy shape, leaf type, and leaf shape) and planting design (individual and in group cluster) were also documented (Table 2). Control Records below the concrete pergola were also recorded. LAI measurements were taken in the afternoon (4-6 PM) when there was no direct sunlight (when the sun was near the horizon). The measurements of LA were performed by Shahidan *et al.* (2010) and from the device catalog (LI-COP-2000).

The sensors' position below the trees' canopy was oriented horizontally in completely shaded locations near the main tree's trunk at 120cm ±10cm from the ground (Figure 2). The time taken to collect the measurements record was approximately one minute.

The UVA (w/m^2) and PAR (lux) measurements were taken at noontime under total sun irradiance (FS_{irrad}) and below the trees' canopy irradiance (BT_{irrad}) on cloudless and sunny days.

Weather conditions in the study area (temperature, relative humidity, and wind speed) were monitored during the measurement days. The temperature ranged between 41.2°C and 45.3°C. Relative humidity ranged between 24 and 47%, while the airspeed was between 1.3 and 5.1 m/s northern, without clouds.

Figure 2: The diagram (A) shows the sun's path and solar zenith angle (θ = 88°-90°) at noontime (12:00–13:00) and the exact period in the year that was applied for all measurements, and (C) shows solar zenith and azimuth in Jeddah, date and hours for data collection (weather spark, 2023). (B) Diagram for tree properties measurements places (tree height H_{tree}, tree canopy diameter D_{canopy}, canopy height H_{canopy}, and trunk height H_{trunk}) and the sensor place for UVA, PAR, and LAI below the trees' canopies.

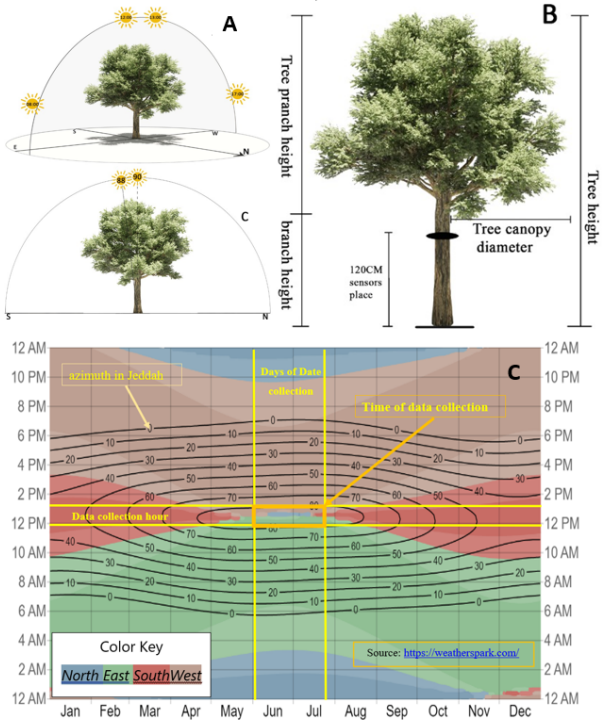

2.3. Equipment and Instruments:

Four instruments were used in the field measurements:

- The visible light (photosynthetically active radiation – PAR) was measured using Li-COR 190SA sensors (LI-COR, Inc., Lincoln, NB), with 400–702 nm response bandwidth.
- Ultraviolet irradiance (UVA) was measured using (a PMA 2110 UVA detector) with a spectral response of 320–400nm (as reported by the manufacturer. The UVA sensor system had a temperature coefficient of <0.1%/C°.
- Leave Area Index (LAI) was measured using LI-COR LAI-2000 Plant Canopy Analysers.
- A digital scale digital clinometer was used to measure the dimensions of the canopies of the trees (H_{tree}, D_{canopy}, H_{canopy}, and H_{branch}).

2.4. Data Processing and Analysis:

The PAR and UVA measurements for various tree canopy species were implemented to obtain the statistical analysis. The relative irradiance (R_{irrad}) for PAR and UVA (R_{PAR} and R_{UVA}) were calculated to estimate the blocking radiation under tree canopy (Grant *et al.*, 2002; Shahidan *et al.*, 2010) with the help of the flowing equation:

$$R_{irrad} = (FS_{irrad} / BT_{irrad}) \text{ X } 100,$$

where FS_{irrad} is the total solar irradiance and BT_{irrad} is the minimum measured irradiance below the tree's canopy at the height of 120 cm near the main tree's trunk at 120 cm (Figure 2).

The means and the standard error of the measurements were also calculated. A comparison model for all SR measurements of PAR and UVA below tree canopies and the characteristics of the tree's canopies (LAI, H_{tree}, D_{canopy}, H_{canopy}, and H_{branch}) was developed.

2.5. Statistical Analyses:

Data for R_{PAR} and R_{UVA} measurement and tree morphological variables (H_{tree}, D_{canopy}, H_{canopy}, and H_{branch}) and LAI were analyzed

using a one-way analysis of variance, ANOVA, to evaluate whether there were significant differences. Post-hoc tests of Least Significant Difference (LSD) were performed to determine the significance of the variation between and within species.

The principal component analysis (PCA) was applied to predict the indirect linear response of R_{PAR} and R_{UVA} and trees' morphological variables. The ordination takes a multivariate dataset of potentially correlated variables and transforms them into fewer uncorrelated variables (principal components). PCA ordination methods are usually fitted by the classical (least squares) regression (Lepš and Šmilauer, 2003). This approach is commonly applied in ecology (Legendre and Legendre 1999). The decision to select the appropriate ordination techniques is made based on gradient length in detrended correspondence analysis (DCA), which estimates the heterogeneity in data; when the gradient length is between 3 and 4, both ordination PCA and correspondence analysis CA is used (Lepš and Šmilauer, 2003). The length in DCA ordination was 3.574, and for that, PCA was used. Hence, the inter-species correlation method (divided by standard deviation) is appropriate for data with significant species turnover across samples (Lepš and Šmilauer, 2003). Significant correlations between PCA axes and R_{PAR} and R_{UVA} were used to evaluate the differences represented by the axes, and species were used as a grouping variable (Deng *et al.*, 2020).

Statistical analyses for one-way variance (ANOVA) were completed using SPSS software for Windows (PASW statistics V22) and PCA using CANOCO software for Windows (Version 4.56).

3. Results

The study of sixty-seven tree samples from eight different species has been completed. The findings show that the trees effectively block PAR and UVA. Furthermore, the characteristics of the trees were thoroughly examined and evaluated, including (LAI, H_{tree}, D_{canopy}, H_{canopy}, and H_{branch}) as shown in (Table 2). The results of this study are promising and suggest that these trees in landscape could reduce the pedestrian effect in urban areas positively.

3.1. Characteristics of Trees' Species:

The mean values measurements of the tree species characteristics were studied. The trees' high H_{tree} for the tallest trees was in the *conoc* (13.1±0.7m), followed by *mill* and *poly* (11.7±1.8m and 11.6m respectively), and the *plu* trees were the shortest samples (5.8±0.5m). As D_{canopy} in the *tab,* trees were the smallest for the diameter of the canopies (1.8±0.3m), but the giant trees were *conoc* (6.5±1m). The height of the canopies, H_{canopy}, was around (4.2±0.3m) in *fnit* and *plu*, while it was more than 11 m for *cono*, *milli*, and *poly*. On the other hand, the tree's branches height H_{branch} of *tab*, *poly*, and *plu* were the shortest trees samples (1.7±0.1, 2±0.1, and 2.1±0.5m respectively), while *conoc* and *mill* were the highest (2.9±0.8 and 3.1±1m), that occurred by pruning of the lower branches in some individuals (Table 3).

Table 3: The mean values ±standard error for PAR, UVA, LAI, and tree dimensions (H_{tree}, D_{canopy}, H_{canopy}, and H_{branch}) of the eight species studied and pergolas.

Species codes	No	PAR	UVA	LAI	D_{canopy}	H_{branch}	H_{tree}	H_{canopy}
cono	7	4.86±1.4	4.53±1.1	3.1±0.2	6.5±0.4	2.9±0.3	13.1±0.7	10.1±0.6
falt	12	2.88±0.5	3.73±0.7	3.5±0.3	5.7±0.3	2.7±0.1	10.1±0.3	7.4±0.3
fnit	12	2.44±0.5	2.37±0.6	2.8±0.2	4.0±0.3	2.5±0.2	6.7±0.3	4.2±0.2
mill	5	8.10±0.7	14.64±2.2	1.4±0.3	3.2±0.4	3.1±0.5	11.7±0.8	9.0±0.8
pelt	15	12.01±1.7	15.60±1.5	1.7±0.2	2.7±0.2	2.3±0.1	8.5±0.4	6.4±0.4
plu	6	5.28±1.6	6.87±2.4	3.1±0.4	2.7±0.3	2.1±0.2	5.8±0.2	4.2±0.1
poly	5	1.26±0.7	1.76±0.9	4.7±1.2	3.3±0.3	2.0±0	11.6±0.6	9.6±0.6
Tab	5	10.52±1	19.48±2	2.9±0.3	1.8±0.1	1.7±0.1	6.7±0.3	5.1±0.3
Total	67	6.11±0.7	8.35±0.9	2.8±0.2	3.9±0.2	2.4±0.1	9.0±0.3	6.7±0.3
Pergola		4.70±3.1	5.91±0.8					

3.2. Leaf Area Index:

LAI mean measurements ranged between 0.33 and 6.26, while the measures of *pelt* and *mill* had the lowest values (1.4±0.3 and 1.7±0.2 respectively), and the measures of *poly* were of the highest value (4.7±1.2) (Table 3).

3.3. PAR and UVA:

The mean values of FS_{irrad} measurements in the study area indicated that the highest record for UVA was 4.64 W/m^2 and for PAR 67500 lux. The R_{PAR} and R_{UVA} for the trees' species showed an apparent variation in their proportions differing by the species. The mean values of the R_{PAR} for tree species ranged from (12.01± 1.7) for *pelt* to (1.26±0.7) for *poly*. However, R_{UVA} ranged from (19.48±2) to (2.37±0.6) for *tab* and *poly*, respectively. On the other hand, the total mean value for R_{UVA} in all species was (8.35±0.9), and for R_{PAR} was (6.11±0.7); in general, the mean values of R_{UVA} were higher than those of R_{PAR}. On the other hand, the total mean value for the pergola R_{PAR} (4.70±3) and R_{UVA} (15.91±0.8). The comparisons between the records of the blocking R_{UVA} and R_{PAR} for tree canopies and concrete pergolas were close to *cocno* and *plu* but were the pergola records higher than *falt*, *fnit*, and *poly*, and were less than the *mill*, *plet*, and *tab* (Table 3).

3.4. ANOVA:

By using a one-way analysis of variance or ANOVA for R_{PAR}, R_{UVA}, and LAI, the results showed a significant variation between species and within species for all trees species (PAR, $F_{df\ 7,\ 59} = 10.044$, $P \leq 0.001$) (UVA, $F_{df\ 7,\ 59} = 22.037$, $P \leq 0.001$) (LAI $F_{df\ 7,\ 59} = 6.7807$, $P \leq 0.001$). The post-hoc multiple compression between species by LSD showed a significant variation of the value of *F,* according to R_{PAR}, R_{UVA}, and LAI. The LSD values of the R_{UVA}, *pelt, tab,* and *mill* trees showed significant differences with all other six species but were not significant among each other. Also, the R_{UVA} *tab* was significant with *conoc*, *fnit*, and *falt,* and the values of *plu* and *poly*. The values of the R_{UVA} *plu* were not significant just with *cono* and *falt*; the R_{UVA} *conoc* were significant with *mill*, *pelt,* and *tab.* On the other hand, for the LSD values of the R_{PAR}, the *tab* showed significant differences with all species except *mill* and *pelt*. The R_{PAR} *poly* was significant with *mill*, *pelt*, and *tab*, and the R_{PAR} *pelt*, was significant for *conoc*, *fnit*, *plu*, and *poly*. Likewise, *mill* values were significant with *fnit*, *falt*, and *poly*; the R_{PAR} for the *plu and cono*; was significant with *pelt* and *tab*. The LSD for LAI values of the *poly* were significant with all species. However, LAI values of the *pelt* showed significant differences with all species except *mill*. Also, *mill* LAI values showed significant differences with all species except *pelt*. The *conoc, fnit,* and *falt* LAI values were significant with a *mill*, *pelt,* and *poly*.

3.5. PCA Analysis:

PCA analysis of the R_{UVA}, R_{PAR}, LAI, and tree morphology for 67 measurements of eight tree species was completed (Figure 3). The first two PCA axes explained 91.6% of the variability. They were significantly correlated, while the cumulative variance percentage of species data for the first two axes were 83.9 and 91.5, respectively (Table 4).

Table 4: PCA ordination diagram summary for the first two axes

Axes	1	2	3	4
Eigenvalues	0.839	0.077	0.055	0.015
Cumulative percentage variance of species data	83.9	91.5	97.0	98.5

The PCA ordination diagram shows a precise type of grouping for the values of the samples and the exact direction of the variable's arrows. The arrows of the R_{PAR} and R_{UVA} were forward to the positive side of axis I, with approximately the same length and slight increase for R_{UVA}. They have effectively contributed to the sample's distribution in

the PCA ordination, as the samples with high values concentrated in the negative side of the first axis, such as (42, 44, 47, 48, 65), while the samples with low values concentrated in the negative side (14, 15, 60, 61, 62) (Figure 3).

Figure 3: PCA ordination diagram for axes I and II displays differentiation between species and variables correlated with each axis

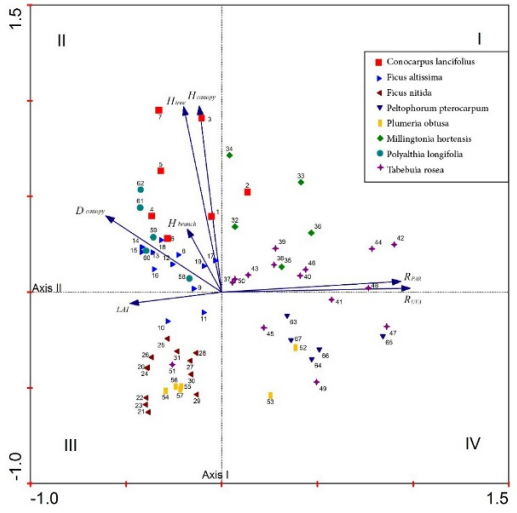

The multiple response curves for the Generalized Linear Model (GLM) of variables for axes I and II with all variables showed different relationships. The response for the LAI, H_{tree}, H_{branch}, H_{canopy}, and D_{canopy} with the axis I was high, while R_{PAR} was lower, followed by R_{UVA}. On the other hand, the response of all variables with axis II was high except the H_{tree} and H_{canopy}, which is less (Figure 4).

Figure 4: The multiple response curves for the generalized linear model (GLM) of variables for axes I and 2 for the PAC ordination diagram.

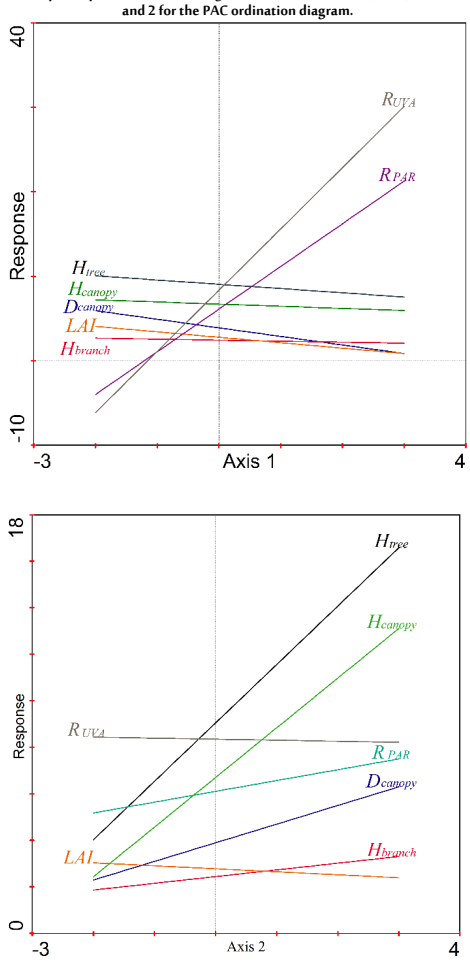

The arrow of the LAI in the PAC ordination diagram was forwarded to the negative side of axis I, which means the tree samples of low values of LAI were concentrated on the positive side of axis I (such as 14, 15, 60, 61, 62, 20, 21, 22, 23, 24, 26, which belong to *poly*, *falt*, and *fnit*) while the high values were on the negative side of axis I (such as 42, 44, 47,48, which belong to *tab*). The arrows of H_{tree}, H_{canopy}, D_{canopy}, and H_{branch} were forward to the positive side of axis II and the negative side of axis I, but the lengths and directions of those arrows were dissimilar. The arrow of the D_{canopy} is oriented towards the negative side of axis I and the positive one from axis II, which is set in the middle between the axes. It concentrated the low values tree samples on the positive side of axis I (such as of 42, 47, 49, and 65 form tab and pelt), while the high values were on the negative side of axis I (such as 3, 4, 5, 7, 61, 62, forming *conoc* and *poly*). In addition, the arrow of the H_{branch} was too short with direction on the positive side of axis II.

Furthermore, the lengths of the arrows of H_{tree} and H_{canopy} were similar and close to the positive side of axis II. Moreover, samples with high values were concentrated on the positive side of axis II (such as 3 and 7 belonging to the *cono*) and low values on the negative side (49, 74, 65, and 48 belonging to the *tab* and *pelt*) (Figure 3).

The distribution of samples for each tree species showed a particular arrangement in the PCA diagram (Figure 3). The *pelt* samples were distributed along the positive side axis I of the ordination in the first and fourth quarters. However, all *mill* samples were accumulated in the first quarter of the ordination. All *conoc* and *poly samples* were collected in the second quarter, and the *falt* samples were concentrated around the ordination center in the second and third quarters. On the other hand, *fnit* and *plu* samples accumulated in the third quarter, while the *tab* samples were concentrated in the fourth.

The sufficient trees for blocking *PAR* and *UVA* radiation were *falt* and *fnit* samples, and the *tab*, *mill*, and *pelt* were the lowest samples; as far as radiation blocking was concerned with the main effect of the LAI values, also the effect of D_{canopy}. These effects were shown in two different cases: the first is when samples were planted as clusters, such as (Samples 14 and 15 of *falt* and 4, 5, and 6 of *conoc*); they have the best values for R_{PAR} and R_{UVA} compared to the samples that were planted separately, such as (Samples 17, 19 of *falt* and 1, 3 *conoc*). The same case occurred for *tab* trees, planted quite apart (Figure 3). The second (which appeared in dense canopy and multilayer trees with pyramid canopy such as *poly* i.e., Samples 61 and 62) was reflected in an apparent increase for R_{PAR} and R_{UVA} than *plu*, which has a low density.

As for the shapes of the leaves, they affected the trees' ability to block radiation, as trees with simple leaves were more efficient in blocking than those with bipinnate leaves. The *falt*, *fnit*, *conoc*, *poly*, and *plu* samples were collected in the second and third quarters, while the *pelt*, *mill*, and *tab* were in the first and fourth quarters. From that, the arrows' positions and directions in the ordination indicate that the trees' canopy characteristics play a prominent role in influencing the proportions of *RPAR* and *RUVA* radiation (Figure 3).

The highest tree values for blocking PAR and UVA were biased towards the second quarter in the diagram, as in the samples of 3 and 7 *conoc* (H_{tree} 15.4, 16 m and H_{branch} 11.6, 12.4 m, respectively). In contrast, the shortest values were collected in the fourth quarter, including 49 and 53 (*tab*=5.2 and *plu*=5 m, respectively).

4. Discussion

The results confirm that the ability of trees to block the PAR and UVA radiation is generally high and better than other types of pergolas. The differences between tree species in achieving the best blocking for PAR and UVA radiation are apparent and related to several variables and

characteristics of each tree such as H_{tree}, H_{branch}, H_{canopy}, D_{canopy}, and LAI.

The most influential variable in blocking PAR and UVA radiation is LAI; the blocking of PAR and UVA would decrease with increased LAI. This case is found in the *poly, fnit,* and *falt* trees with the highest radiation blocking. Their multi-layered crown and dense leaves distinguish these trees. That result was appropriate for researchers who have studied the effect of LAI on other types of SR (such as thermal radiation) (Armson *et al.*, 2013; Zhang *et al.*, 2018; Rahman *et al.*, 2018).

LAI is a seasonally variable dynamic feature that affects many conditions such as environmental conditions, tree health, agricultural maintenance, and planting design. It can, however, be changed and improved over time by agricultural and environmental treatments and individual tree species (Sanusi *et al.*, 2017).

The canopy diameter is also essential in influencing the blocking of PAR and UVA. It is increased with a high-value diameter, such as *conoc,* than with a small diameter such as *tab* and *plu.* Many researchers (De-Abreu-Harbich *et al.*, 2015; Armson, 2013; Zhang *et al.,* 2018; Kwon and Lee, 2019) have indicated that the efficiency of blocking SR increases with the canopies' diameter.

The leaf's shape and size significantly affect PAR and UVA. Large and simple leaves, such as those of *conoc, poly, fnit,* and *falt* can block PAR and UVA better than small and compound leaves (bipinnate) such as those of *pelt* and *mill* (Figure 3). The role of the leaf shape has been indicated as influencing SR in both (De-Abreu-Harbich *et al.*, 2015; Sanusi *et al.*, 2017).

Again, the shapes of canopies influenced PAR and UVA as trees such as *poly* (pyramid shapes) and *fnit* (rounded shape) were the most efficient in blocking PAR and UVA. However, the oblong-shaped trees such as *tab* and *conoc* were the least efficient (Figure 3).

The results indicate that the blocking of PAR and UVA increased when the tree cover density was increased by cluster (group or rows) compared to individual trees without overlapping canopy. This case was seen clearly in many situations (*pelt, conoc,* and *falt*) when trees were planted in clusters. Thus, clusters of trees can influence the sunrays and modify the properties of the micro-climate better than individual trees (De-Abreu-Harbich *et al.*, 2015). Therefore, increasing tree density in urban areas can positively change local climatic and health perspectives (Salmond *et al.*, 2016).

The comparison between the tall trees (H_{tree}) (such as *conoc* and *mill*) and small trees (such as *tab* and *plu*) and Canopy height trees (H_{canopy}) (such as *conoc*, *mill*, and *falt*) reasonable; when the height and canopy of the tree increase the effect of blocking PAR and UVA also increases. This result is consistent with what was stated by (Smithers *et al.*, 2018) about replacing large trees with small ornamental trees to mitigate the heat islands in cities.

Removing the lower branches of trees, which increased the branches' height (H_{branch}), affected their ability to block the PAR and UVA and increased the LAI values because of the increased quantity of radiation from the sides. These cases were noticeable in many species' samples such as *pelt* and *conoc*.

The ability of trees to block out PAR and UVA increases at different levels when more than one characteristic of the essential variables of the tree are combined, including low values of LAI, multilayers of the tree and with simple leaves, big and large diameter tree as well as maintaining a short tree's trunk and planting trees in clusters.

The characteristics of tree canopy such as shape, height, diameter, or leaf shape were often continuously available to urban planners and landscape architecture designers. They can be essential in selecting species for the landscape architecture project.

5. Conclusion

In our research paper, we delved into various tree features that can be utilized to block solar radiation in urban environments. We studied eight tree species commonly used in landscape architecture, to determine their effectiveness in blocking UVA and PAR radiation in urban areas. The study was conducted on the campus of King Abdulaziz University, situated in the central-west part of Saudi Arabia. The measurements were taken at a specific time, noontime (12:00–13:00) when the solar zenith angle was perpendicular (θ = 88°–90°) from 01-June to 15-July. The results revealed that trees were effective in blocking PAR and UVA. The trees' characteristics (LAI, H_{tree}, H_{branch}, H_{canopy}, and D_{canopy}) play an essential role in blocking PAR and UVA. Factors such as trees' shape, the shapes and sizes of leaves, agricultural maintenance, and planting design have various impacts on blocking PAR and UVA. Finally, the shades of the trees are essential to reduce and protect humans from PAR and UVR in an arid region. Trees also improve the quality of life, especially in the urban environment, by providing aesthetic and environmental benefits to the urban environment.

Biography

Abdullah M. Farid Ghazal

Department of Landscape Architecture, Faculty of Architecture and Planning, King Abdulaziz University, Jeddah, Saudi Arabia, 00966506620717, aghazal@kau.edu.sa

Ghazal holds a Ph.D. in Landscape ecology and biodiversity from Hohenheim University, Germany. He is an associate professor at the Department of Landscape Architecture at the Faculty of Architecture and Planning at KAU, KSA. Before, he worked full-time at Aleppo University, Syria, (KACST) KSA, and part-time at (ACSAD). He has published 28 papers and won several awards in landscape architecture projects as an ecological consultant. The current research interest concerns landscape ecology, biodiversity, plant material, and design in LA, especially in an arid region.

ORCID: 0000-0001-6890-4717

References

Armson, D., Rahman, M.A. and Ennos, A.R. (2013). A comparison of the shading effectiveness of five different street tree species in Manchester, UK. *Arboriculture and Urban Forestry*, **39**(4), 157–64. DOI: 10.48044/jauf.2013.021

Boukelia, T.E., Mecibah, M.S. and Meriche, E.D. (2014). General models for estimation of the monthly mean daily diffuse solar radiation (Case study: Algeria). *Energy Conversion and Management,* **81**(n/a), 211–9. DOI: 10.1016/j.enconman.2014.02.035

Cancer Research UK. (2021). *How Does the Sun and UV Cause Cancer*? Available at: https://www.cancerresearchuk.org/about-cancer/causes-of-cancer/sun-uv-and-cancer/how-does-the-sun-and-uv-cause-cancer. (accessed on 21 /12/ 2022).

De-Abreu-Harbich, L.V., Labakia, L.C. and Matzarakisb, A. (2015). Effect of tree planting design and tree species on human thermal comfort in the tropics. *Landscape and Urban Planning*, **138**(n/a), 99–109. DIO: 10.1016/j.landurbplan.2015.02.008

Deng J., Pickles, B.J., Smith, S.T. and Shao, L. (2020). Infrared radiative performance of urban trees: spatial distribution and interspecific comparison among ten species in the UK by in-situ spectroscopy. *Building and Environment*, **172**(n/a), 106682. DIO: 10.1016/j.buildenv.2020.106682

Environment, Health & Safety. (2018). *Light and Infrared Radiation.* Available at: https://ehs.lbl.gov/resource/documents/radiation-protection/non-ionizing-radiation/light-and-infrared-radiation/. (accessed on 30 /09/ 2022).

Fahmy, M., Sharples, S. and Yahiya, M. (2010). LAI based trees selection for mid latitude urban developments: A microclimatic study in Cairo, Egypt. *Building and Environment*, **45**(2), 345–57. DOI: 10.1016/j.buildenv.2009.06.014

Fuller, K.K., Loros, J.J. and Dunlap, J.C. (2015). Fungal photobiology: visible light as a signal for stress, space and time. *Current Genetics*, **61**(n/a), 275–88. DOI: 10.1007/s00294-014-0451-0

Gies, P. and Mackay, C. (2004). Measurements of the Solar UVR protection provided by shade structures in New Zealand Primary Schools. *Photochemistry and Photobiology*, **80**(2), 334–9. DOI: 10.1111/j.1751-1097

Gies, P. and Wright, J. (2003). Measured solar ultraviolet radiation exposures of outdoor workers in Queensland in the building and construction industry. *Photochemistry and Photobiology*, **78**(4), 342–8. DOI: 10.1562/0031-8655

Grant, R.H. and Heisler, G.M. (2001). Multi-waveband solar irradiance on tree-shaded vertical and horizontal surfaces: Cloud-free and partly cloudy skies. *Photochemistry and Photobiology*, **73**(1), 24–31. DOI: 10.1562/0031-8655

Grant, R.H. and Heisler, G.M. (2006). Effect of cloud cover on UVB exposure under tree canopies: Will climate change affect UVB exposure? *Photochemistry and photobiology*, **82**(2), 487–94. DOI: 10.1562/2005-07-07-RA-604

Grant, R.H., Heisler, G.M. and Gao, W. (2002). Estimation of pedestrian level UV exposure under trees. *Photochemistry and Photobiology*, **75**(4), 369–76. DOI: 10.1562/0031-8655

Grant, R.H., Heisler, G.M., Gao, W. and Jenks, M. (2003). Ultraviolet leaf reflectance of common urban trees and the prediction of reflectance from leaf surface characteristics. *Agricultural and Forest Meteorology*, **120**(1-4), 127–39. DOI: 10.1016/j.agrformet

Heisler, G.M., Grant, R.H. and Gao, W. (2003). Individual-and scattered-tree influences on ultraviolet irradiance. *Agricultural and Forest Meteorology*, **120**(1-4), 113–26. DOI: 10.1016/j.agrformet

Heisler, G.M., Grant, R.H., Gao, W. and Slusser, J.R. (2004). Solar Ultraviolet-B Radiation in Urban Environments: The Case of Baltimore, Maryland. *Photochemistry and Photobiology*, **80**(3), 422–8. DOI: 10.1111/j.1751-1097

Kong, L., Lau, K.K.L., Yuan, C., Chen, Y., Xu, Y., Ren, C. and Ng, E. (2017). Regulation of outdoor thermal comfort by trees in Hong Kong. *Sustainable Cities and Society*, **31**(n/a), 12–25. DOI: 10.1016/j.scs.2017.01.018

Kwon, Y.J. and Lee, D.K. (2019). Thermal comfort and longwave radiation over time in urban residential complexes. *Sustainability*, **11**(8), 2251. DOI: 10.3390/su11082251

Legendre, P. and Legendre, L. (1998). *Numerical Ecology*. 2nd edition. Amsterdam: Elsevier.

Lepš, J. and Šmilauer, P. (2003). *Multivariate Analysis of Ecological Data Using CANOCO*. United Kingdom: Cambridge University Press.

Modenese, A., Bisegna, F., Borra, M., Grandi, C., Gugliermetti, F., Militello, A. and Gobba, F. (2016). Outdoor work and solar radiation exposure: Evaluation method for epidemiological studies. *Medycyna Pracy*, **67**(5), 577-587. DOI: 10.13075/mp.5893.00461

Modenese, A., Korpinen, L. and Gobba, F. (2018). Solar radiation exposure and outdoor work: An underestimated occupational risk. *International Journal of Environmental Research and Public Health*, **15**(10), 2063. DOI: 10.3390/ijerph15102063

Morakinyo, T.E., Dahanayake, K.K.C., Adegun, O.B. and Balogun, A.A. (2016). Modelling the effect of tree-shading on summer indoor and outdoor thermal condition of two similar buildings in a Nigerian university. *Energy and Buildings*, **130**(n/a), 721–32. DOI: 10.1016/j.enbuild.2016.08.087

Parker, J. and Simpson, G.D. (2020). A case study balancing predetermined targets and real-world constraints to guide optimum urban tree canopy cover for Perth, Western Australia. *Forests*, **11**(11), 1128. DOI: 10.3390/f11111128

Rahman, M.A., Moser, A., Gold, A., Rötzer, T. and Pauleit, S. (2018). Vertical air temperature gradients under the shade of two contrasting urban tree species during different types of summer days. *Science of the Total Environment*, **633**(n/a), 100–11. DOI: 10.1016/j.scitotenv

Salmond, J.A., Tadaki, M., Vardoulakis, S., Arbuthnott, K., Coutts, A., Demuzere, M., Dirks, K.N., Heaviside, C., Lim, S., Macintyre, H., McInnes, R.N. and Wheeler, B.W. (2016). Health and climate related ecosystem services provided by street trees in the urban environment. *Environmental Health*, **15**(1), 95–111. DOI: 10.1186/s12940-016-0103-6

Sanusi, R., Johnstone, D., May, P. and Livesley, S.J. (2017). Microclimate benefits that different street tree species provide to sidewalk pedestrians relate to differences in Plant Area Index, *Landsc. Urban Planning*, **157**(n/a), 502–11. DOI: 10.1016/j.landurbplan

Shahidan, M.F., Shariff, M.K.M., Jones, P., Salleh, E. and Abdullah A.M. (2010). A comparison of *Mesua ferrea* L. and *Hura crepitans* L. for shade creation and radiation modification in improving thermal comfort. *Landscape and Urban Planning*, **97**(3), 168–81. DOI: 10.1016/j.landurbplan

Smithers, R.J., Doick, A.B., Burton, A., Sibille, R., Steinbach, D., Harris, R., Groves, L. and Blicharska, M. (2018). Comparing the relative abilities of tree species to cool the urban environment. *Urban Ecosystems*, **21**(n/a), 851–62. DOI: 10.1007/s11252-018-0761-y

Trumbull, D.J. and Parisi, A.V. (2010). Latitudinal Variations over Australia of the Solar UV-Radiation Exposures for Vitamin D3 in Shade Compared to Full Sun. *Radiation Research*, **173**(3), 73–379. DOI: 10.1667/RR1951.1

TUN, K. and MG, T. (2020). Temperature reduction in urban surface materials through tree shading depends on surface type not tree species. *Forests*, **11**(11), 1141. DOI: 10.3390/f11111141

Weather Spark. (2023). *The Weather Year Round Anywhere on Earth*. Available at: https://weatherspark.com. (accessed on 20 /09/ 2023).

World Healthy Organization. (2016). *Radiation: Ultraviolet (UV) Radiation*. Available at: https://www.who.int/news-room/q-a-detail/radiation-ultraviolet-(UV). (accessed on 30 /01/ 2023).

Yeo, L., Ling, G., Tan, M. and Leng, P. (2021). Interrelationships between land use land Cover (LULC) and human thermal comfort (HTC): A Comparative Analysis of Different Spatial Settings. *Sustainability*, **13**(1), 382. DOI: 10.3390/su13010382

Zhang, L., Zhan, Q. and Lan, Y. (2018). Effects of the tree distribution and species on outdoor environment conditions in hot summer and cold winter zone: A case study in Wuhan residential quarters. *Building and Environment*, **130**(n/a), 27–39. DOI: 10.1016/j.buildenv

Zhao, Q., Yang, J., Wang, Z.H. and Wentz, E.A. (2018). Assessing the cooling benefits of tree shade by an outdoor urban physical scale model at Tempe, AZ. *Urban Science*, **2**(1), 4. DOI: 10.3390/urbansci2010004

Zheng, S., Guldmann, J.M., Liu, Z. and Zhao, L. (2018). Influence of trees on the outdoor thermal environment in subtropical areas: An experimental study in Guangzhou, China. *Sustainable Cities and Society*, **42**(n/a), 482–97. DOI: 10.1016/j.scs.2018.07.025